Supporting Information

Built-in electric field coupled with non-noble metal plasma cocatalyst boosts photocatalytic CO_2 reduction of MIL-125

Xiaokang Jiang [a1], Yongze Gao [a1], Bowen Zhang [a1], Xiaodong Yang [a], Zhimin Yuan [b,*], Zhaoning Xu [a], Bin Sun [c,*], Zaiyong Jiang [b], Guowei Zhou [c,*], Enlong Zhou [a,*]

[a] *College of Chemistry and Material Science, Shandong Agricultural University, Taian, 271018, Shandong, PR China*

[b] *School of Chemistry & Chemical Engineering and Environmental Engineering, Weifang University, Weifang, Shandong, 261061, P.R. China*

[c] *School of Chemistry and Chemical Engineering, Qilu University of Technology (Shandong Academy of Sciences), Jinan 250353, Shandong, China*

*Corresponding authors:

E-mail: yuanzhiminjinan@163.com; binsun@qlu.edu.cn; gwzhou@qlu.edu.cn; chemelzhou@sdau.edu.cn;

[1] Contributed equally to this work.

Materials

Tetrabutyl titanate (TBOT) ($C_{16}H_{36}O_4Ti$, 98.0 %) and Titanium oxide (TiO_2, 99.0 %) were purchased from Aladdin Biochemical Technology Co. Ltd. Methanol (CH_3OH, ≥99.5 %) was purchased from Kaitong Chemical Reagent Co. Ltd. N, N-Dimethylformamide (C_3H_7NO, DMF, ＞99.90 %), terephthalic acid ($C_8H_6O_4$, ＞99 %) and Bismuth nitrate pentahydrate ($Bi(NO_3)_3·5H_2O$, 99 %) were purchased from Macklin Biochemical Technology Co. Ltd, All the chemicals were used as received without further purification.

Material characterizations

The crystalline phases were analyzed by an X-ray diffraction (XRD) instrument (SmartLab SE) under Cu Kα radiation (λ = 1.540590 Å) within the 2θ range of 5° to 80°. The accelerating voltage and applied current were 40 kV and 30 mA, respectively, and the scan rate was $5°·min^{-1}$. Scanning electron microscopy (SEM) images were obtained by Regulus 8100 at an acceleration voltage of 5 kV. Transmission electron microscopy (TEM) images were obtained by a JEOL TEM instrument at the accelerating voltage of 200 kV. The Brunauer Emmett Teller (BET) surface areas were measured by nitrogen adsorption isotherm measurements at 77 K on a 3H-2000PS2 instrument. Fourier transform infrared (FT-IR) spectra were recorded on a Bruker TENSOR II spectrometer in the range of 400-4000 cm^{-1} using KBr pellets. The UV-vis diffuse reflectance spectra (UV-vis DRS) were obtained for the dry-pressed disk samples using a Cary 500 Scan UV-vis spectrophotometer (Varian). Electron paramagnetic resonance (EPR, Bruker- A300) was used to investigate oxygen vacancies on samples. In situ X-ray photoelectron spectra and X-ray photoelectron spectra (XPS) were collected with a Thermo Scientific ESCALAB 250Xi X-ray photoelectron spectrometer. All binding energies were calibrated using C 1s at 284.8 eV as a reference. Steady-state fluorescence spectrum and transient fluorescence spectrum were studied by Edinburgh FLS1000. In-situ FT-IR (DRIFTS) spectra were acquired on a Thermo Scientific Nicolet iS50 FT-IR spectrometer equipped with an in-situ DRIFTS cell supplied by Hefei In-situ Technology Co., Ltd. (Hefei, China).

Photoelectrochemical measurements

Mott-Schottky plots (M-S), transient photocurrent measurements and electrochemical impedance spectroscopy measurements (EIS) were obtained on a CHI 760E electrochemistry workstation with a

standard three-electrode system, in which the sample-coated ITO was used as working electrode, and platinum-wire electrode and Ag/AgCl electrode were used as counter electrode and reference electrode, respectively. In this three-electrode system, 0.2 M Na_2SO_4 was selected as the electrolyte. The working electrode is prepared as follows: 5 mg of photocatalyst is dispersed in 1 mL of EtOH by ultrasound, and drop-coated onto clean and smooth working electrode (1×5 cm) that have been cleaned with water, ethanol, and acetone by ultrasound. Finally, the electrode is dried overnight at 60 ℃ in a vacuum oven to obtain the working electrode. And a 300 W Xeon lamp was employed as the light source.

Photocatalytic CO_2 reduction

The photocatalytic CO_2 reduction measurement was carried out in a 180 mL gastight photoreactor with a quartz plate at the top and sampling ports at two sides. Typically, 5 mg of photocatalysts were ultrasonically dispersed in 2 mL of deionized water and then uniformly coated on a glass slide. After dried appropriately, the glass slide was fixed in the reactor with 1.7 mL ultrapure water filling the bottom. The air in the reactor was completely removed by a vacuum pump. Subsequently, high purity CO_2 (99.999 %) was first passed through ultrapure water to carry water vapor before being introduced into the reactor. This process was repeated for 3 times. Finally, the reactor was then irradiated under a 300 W Xe lamp (PLS-SXE300E, Beijing Perfect Light, China) equipped with a power density of 150 mW cm^{-2}. The circulating cooling water system was used to keep the reaction temperature at 25 °C. The generated products were periodically analyzed by a gas chromatograph (HF-901A, HuiFen, China) equipped with both thermal conductivity detector (TCD) and flame ionization detector (FID).

Theoretical calculation methods

Density functional theory calculations with the Perdew-Burke-Ernzerhof (PBE) functional were carried out with Quantum ESPRESSO version 7.2. Standard solid-state pseudopotentials were used. The kinetic energy cutoff for plane-wave wavefunctions was set to 50 Rydberg, and the kinetic energy cutoff for charge density and potential was set to 450 Rydberg. Gaussian smearing with a width of 0.02 Rydberg for brillouin-zone integration was applied. Grimme's D3 dispersion correction with Becke-Johnson damping was included. Monkhorst-Pack 4×4×1 K-point grids were used. A vacuum space of 30 Å along the z direction was used between adjacent layers. Charge transfer was quantified by Bader charge analyses.

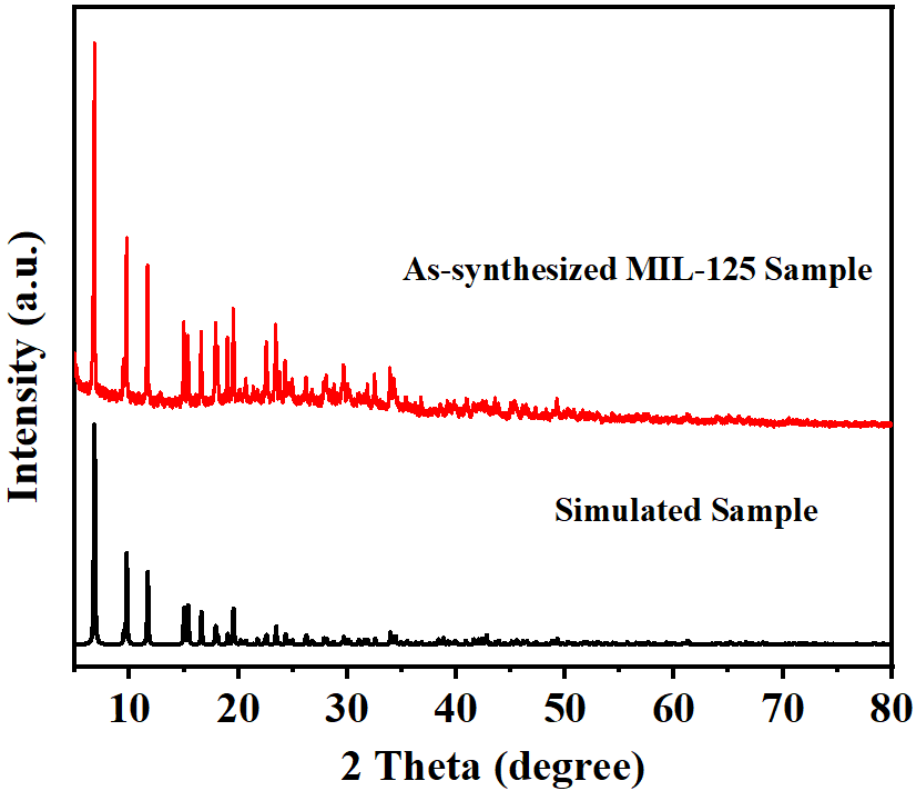

Fig. S1. The XRD pattern of synthesized and the simulated MIL-125.

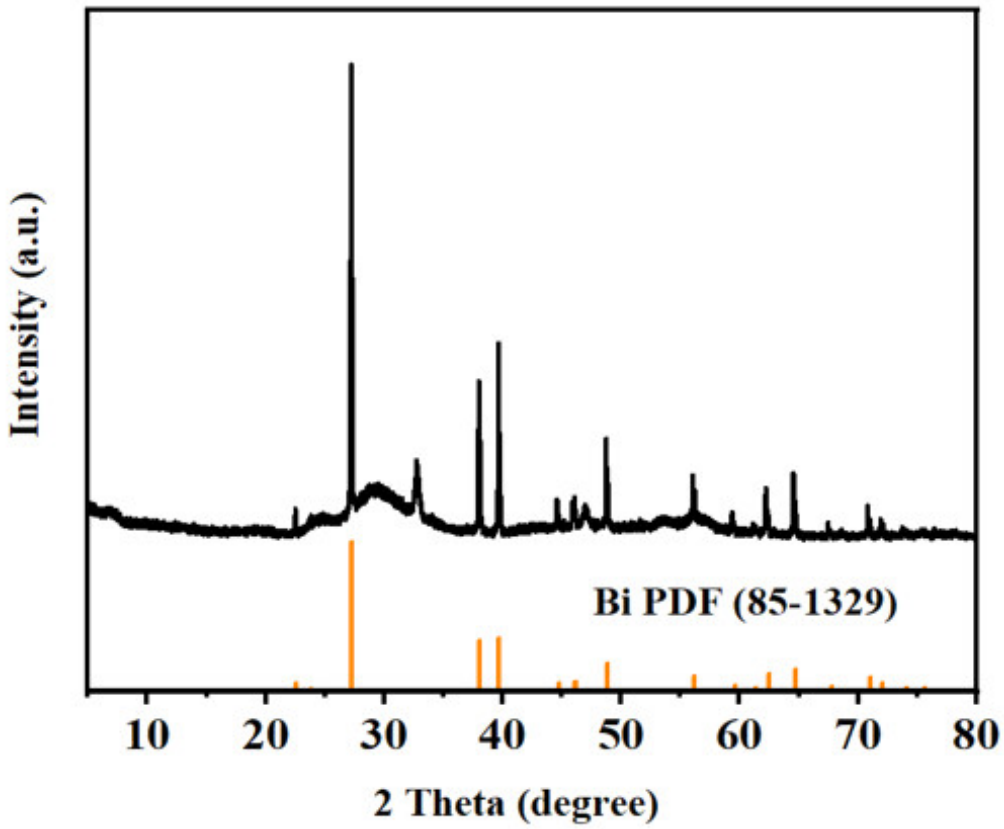

Fig. S2. XRD pattern of pure metal Bi.

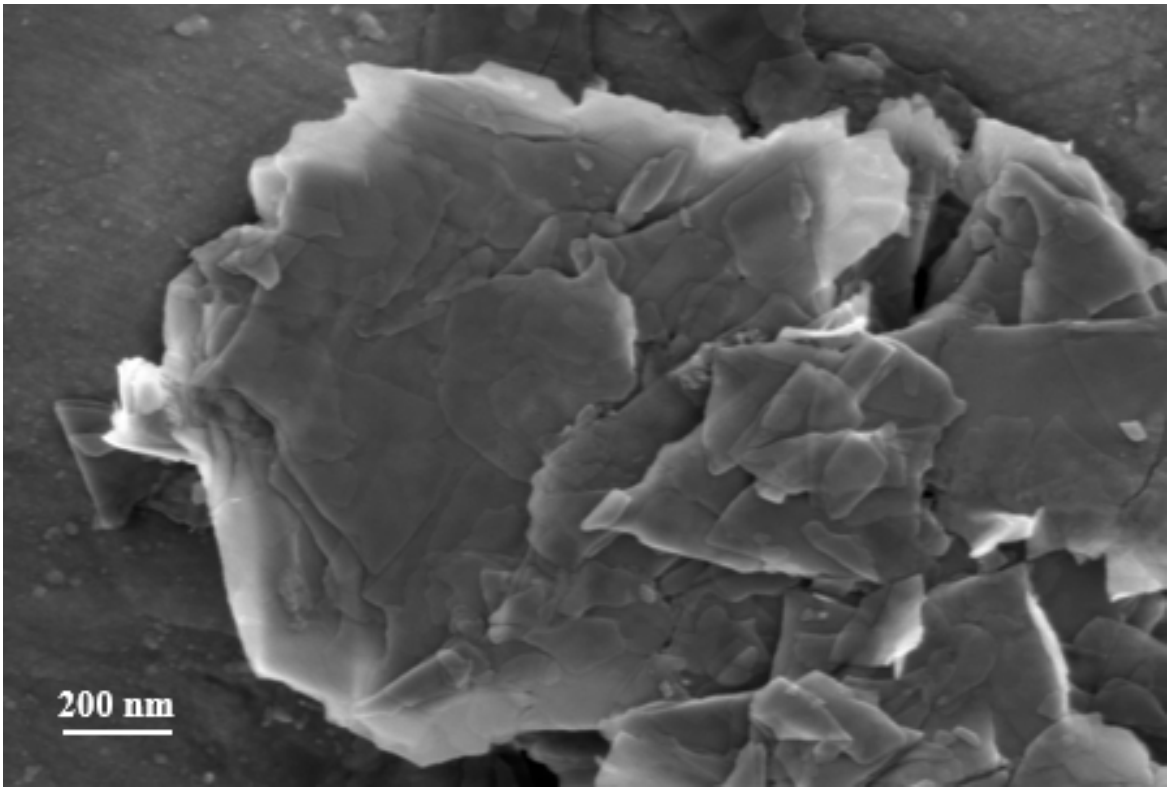

Fig. S3. SEM of pure metal Bi.

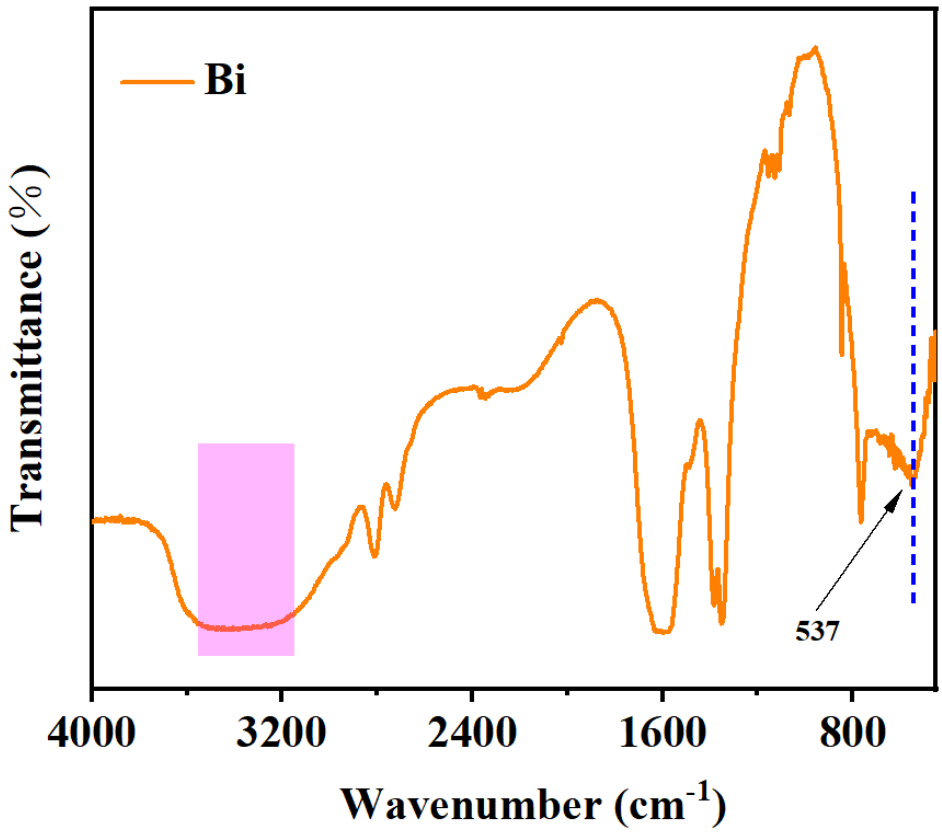

Fig. S4. The FT-IR of pure metal Bi.

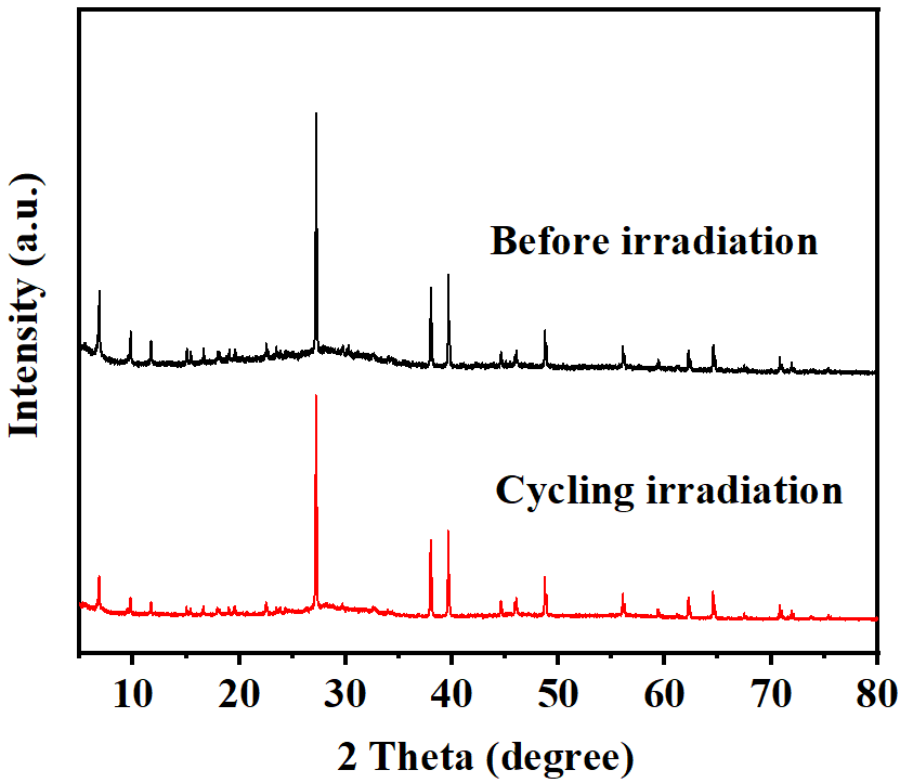

Fig. S5. The XRD of BM-110 before irradiation and after cyclic irradiation.

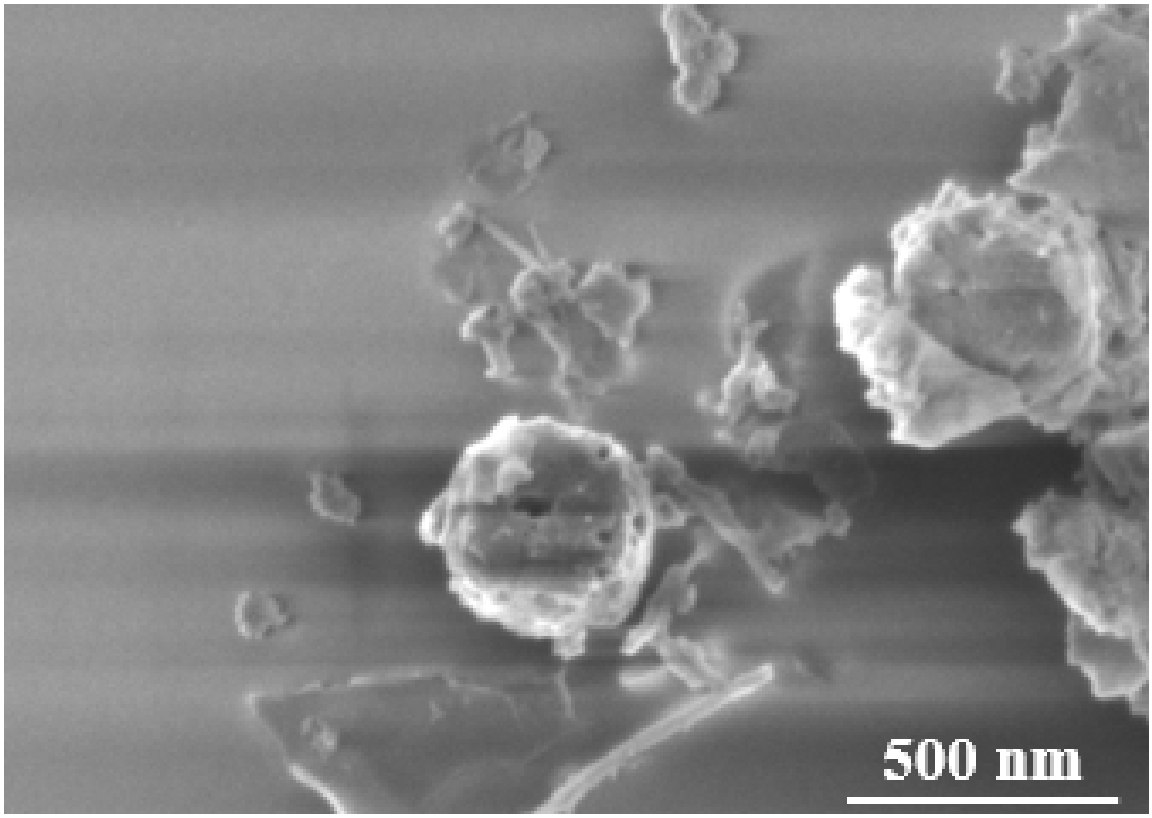

Fig. S6. The SEM of cycling irradiation.

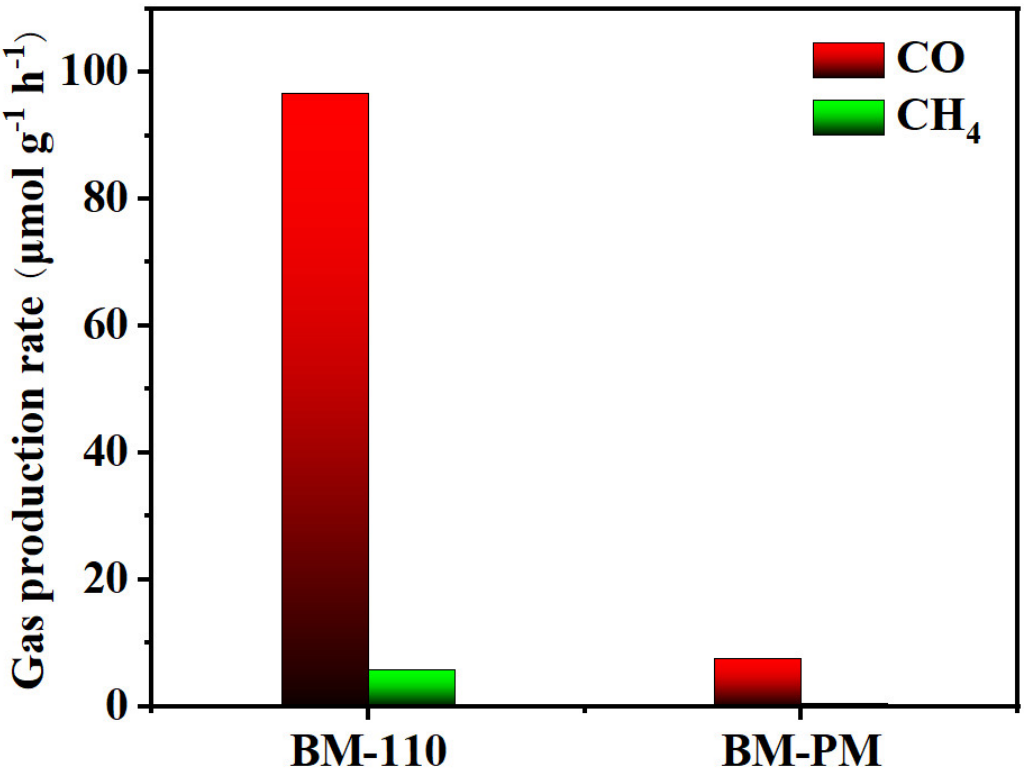

Fig. S7. The performance comparison of BM-110 and BM-PM.

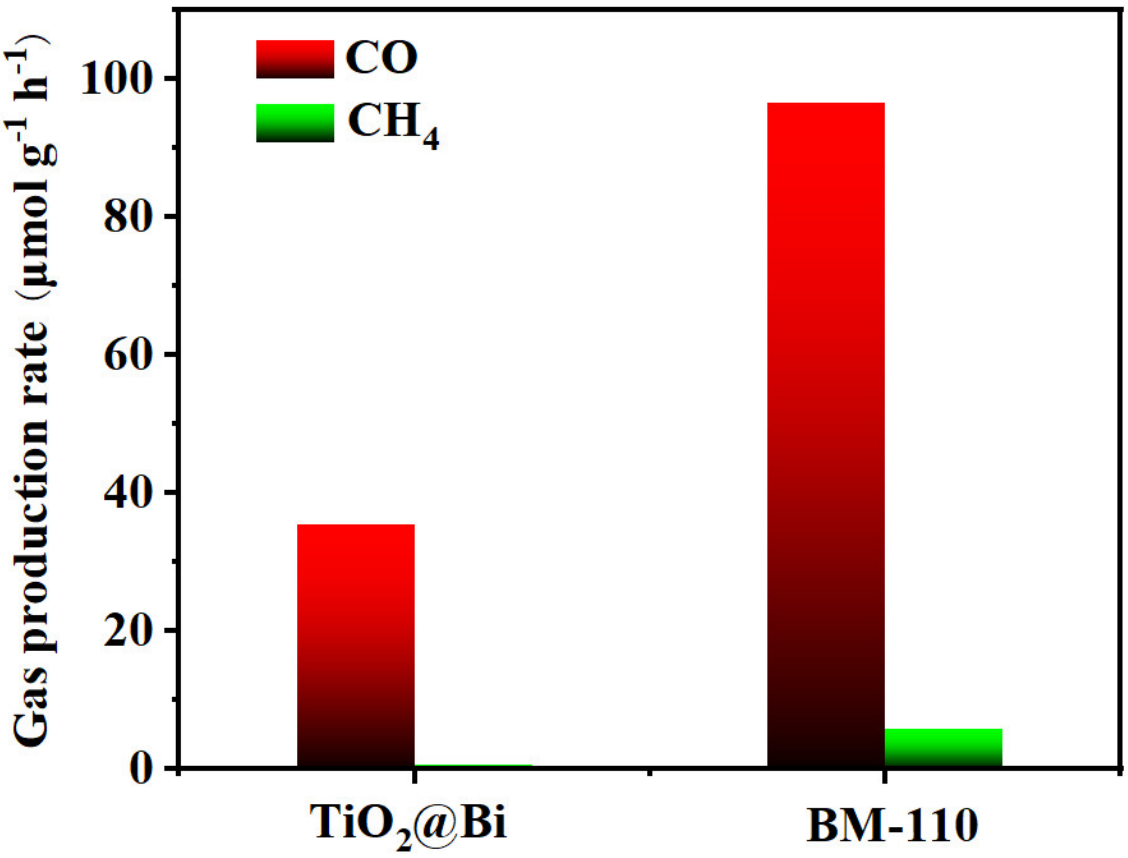

Fig. S8. Performance comparison between commercial TiO_2 loaded Bi NPs and BM-110.

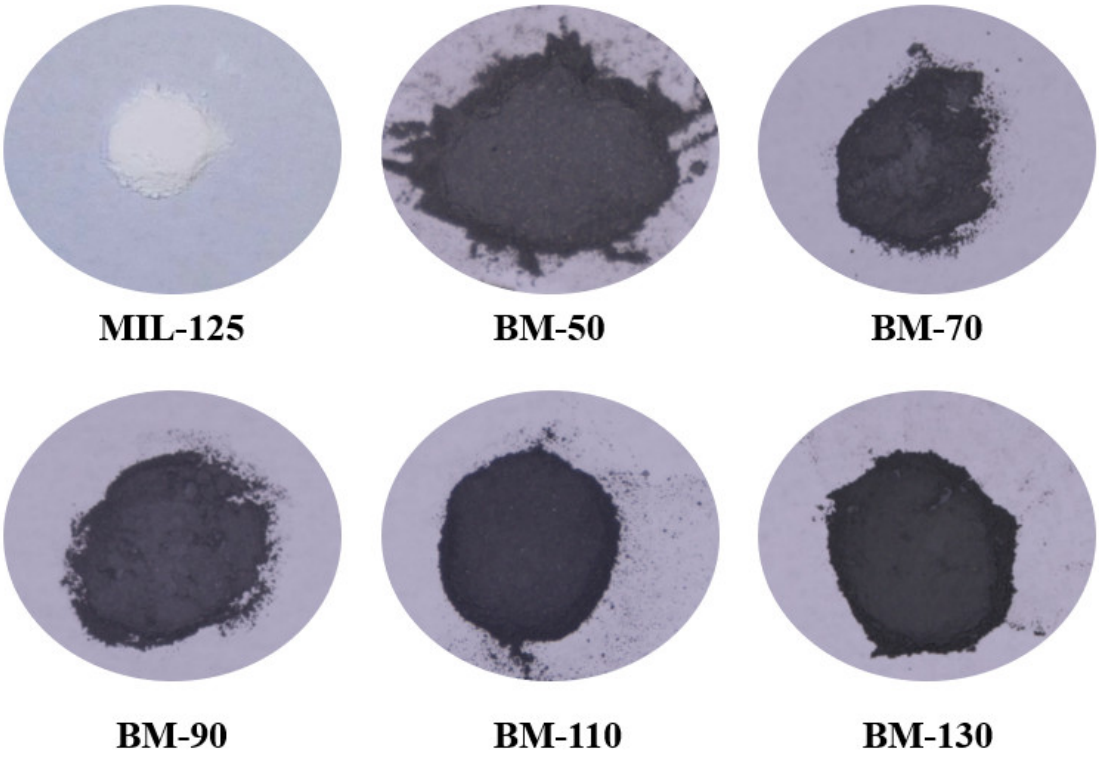

Fig. S9. The colors of as-prepared samples.

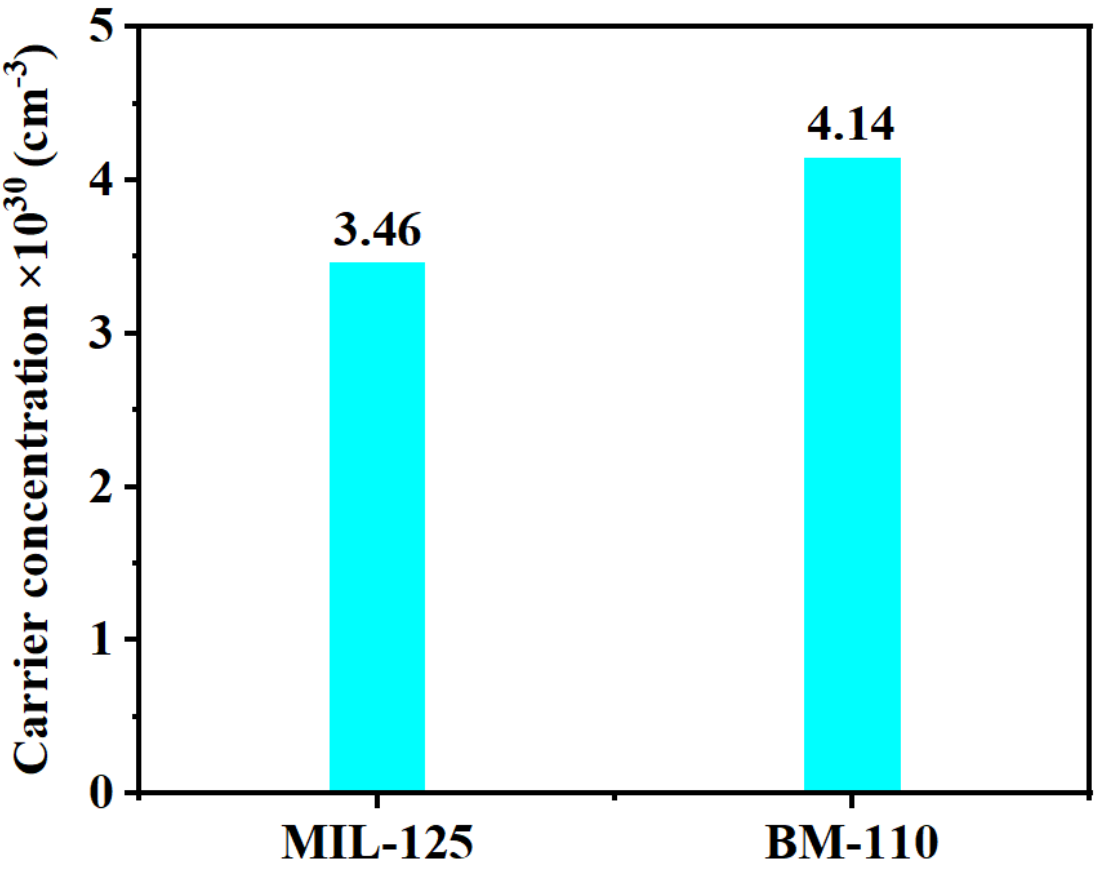

Fig. S10. The carrier concentration of MIL-125 and BM-110.

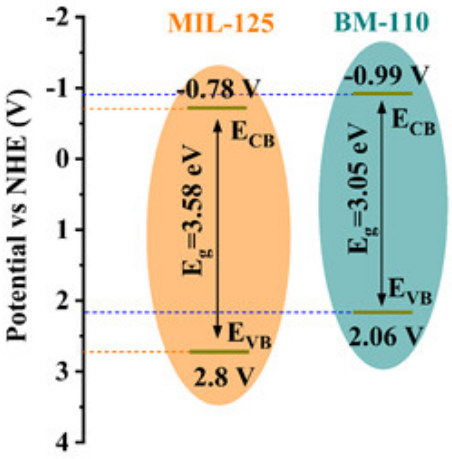

Fig. S11. The band position of MIL-125 and BM-110.

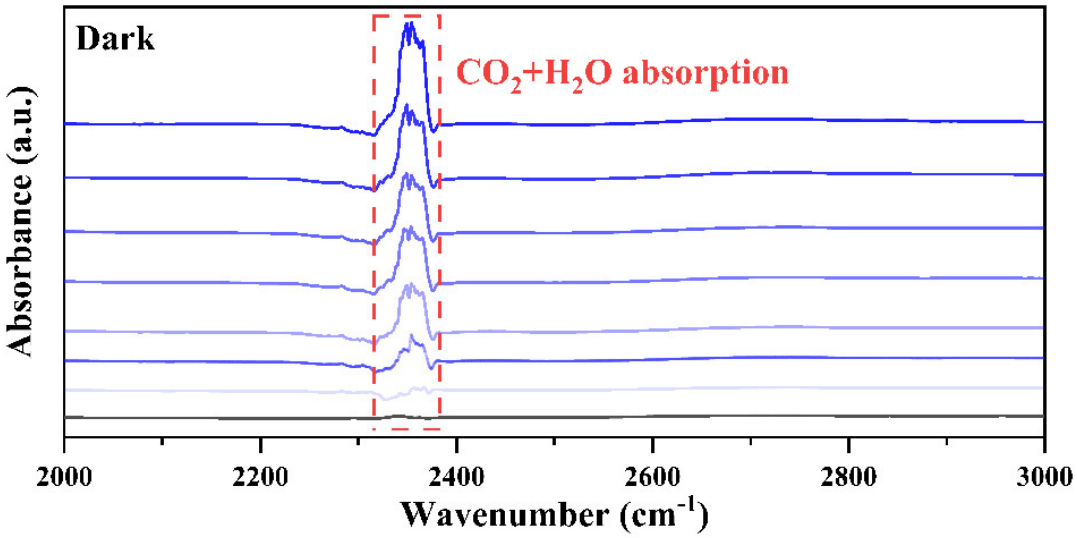

Fig. S12. In situ infrared spectra of BM-110 under dark conditions.

Table S1. Surface area, pore size, and pore volume parameters for various materials.

Sample	Surface area [a] (m^2/g)	Pore size [b] (nm)	Vt [c] (cm^3/g)
MIL-125	1621.38	1.1	0.77
BM-110	297.31	5.98	0.45

a: BET Surface Area

b: Adsorption average pore diameter

c: Single point adsorption total pore volume of pores

Table S2. The surface element composition of MIL-125 and BM-110.

Element	MIL-125	BM-110
C 1s	64.04%	44.52%
O 1s	29.13%	32.49%
Ti 2p	6.82%	16.32%
Bi 4f	-	6.67%

Table S3. Comparison of BM-110 performance with other catalysts.

Catalytic	Light	Reaction medium	Products	Photocatalytic efficiencis ($\mu mol\ g^{-1}\ h^{-1}$)	Ref.
InO/Bi/BOC-4	300W Xe lamp	CO_2 + pure H_2O	CO	34.53	[1]
UiO-66-NH_2-Zn SAS	300W Xe lamp	CO_2 + pure H_2O	CO	40.23	[2]
5 % M/BMO	300W Xe lamp	$NaHCO_3$ + H_2SO_4	CO	25.21	[3]
Pd/Bi-MOF	300W Xe lamp	CO_2 + pure H_2O	CO	20.33	[4]
V_{Bi}-BiOBr	300W Xe lamp	CO_2 + pure H_2O	CO	20.1	[5]
BM-110	300W Xe lamp	CO_2 + pure H_2O	CO	96.63	This work

References

[1] K. Wang, T. Sun, H. Ma, R. You, Z. He, J. Chen, H. Wang, W. Wang, Y. Yang, L. Wang, Z. Liu, *Sep. Purif. Technol.*, **2024**, 340, 126786.

[2] M. Chu, Y. Li, X. Chen, G. Hou, Y. Zhou, H. Kang, W. Qin, X. Wu, *J. Mater. Chem. A,* **2022**, 10, 23666-23674.

[3] L. Liu, K. Dai, J. Zhang, L. Li, *J. Colloid Interf. Sci*., **2021**, 60, 4844-855.

[4] C. Ma, Z. Zhong, Q. Xiang, *Mol. Catal.* **2025**, 571, 114700.

[5] Z. Li, Y. Rong, J. Liang, Z. Li, J. Wei, J. Li, S. Zhang, T. Liang, Z. Yu, Y. Hou, *J. Environ. Chem. Eng.*, **2022**, 10, 108819.